4-1-1987

Studies on the Ultrastructure of Fibrin Lacking Fibrinopeptide B (β-Fibrin)

Michael W. Mosesson
Blood Center of Wisconsin

James P. DiOrio

Michael Muller
IBM Research

John R. Shainoff
Baxter Healthcare Corp.

Kevin R. Siebenlist
Marquette University, kevin.siebenlist@marquette.edu

See next page for additional authors

Blood, Vol. 69, No. 4 (April 1987): 1073-1081. DOI.

Studies on the Ultrastructure of Fibrin Lacking Fibrinopeptide B (β-Fibrin)

M.W. Mosesson
Mount Sinai Medical Center, University of Wisconsin Medical School, Milwaukee Clinical Campus, Marl, FRG
J.P. DiOrio
Mount Sinai Medical Center, University of Wisconsin Medical School, Milwaukee Clinical Campus, Marl, FRG
M.F. Müller
Hüls-AG, Marl, FRG
J.R. Shainoff
Cleveland Clinic, Research Division, Paris
K.R. Siebenlist
Mount Sinai Medical Center, University of Wisconsin Medical School, Milwaukee Clinical Campus, Marl, FRG
D.L. Amrani

Mount Sinai Medical Center, University of Wisconsin Medical School, Milwaukee Clinical Campus, Marl, FRG

G.A. Homandberg

Mount Sinai Medical Center, University of Wisconsin Medical School, Milwaukee Clinical Campus, Marl, FRG

J. Soria

Laboratoire Central d'Hèmatologie, Hôtel-Dieu de Paris, Paris

C. Soria

Laboratoire Central Biochim Hematologic Hôpital Lariboisière, Paris

M. Samama

Laboratoire Central d'Hèmatologie, Hôtel-Dieu de Paris, Paris

Release of fibrinopeptide B from fibrinogen by copperhead venom procoagulant enzyme results in a form of fibrin (*β*-fibrin) with weaker self-aggregation characteristics than the normal product (*β*-fibrin) produced by release of fibrinopeptides A (FPA) and B (FPB) by thrombin. We investigated the ultrastructure of these two types of fibrin as well as that of *β*-fibrin prepared from fibrinogen Metz (Aα16 Arg→Cys), a homozygous dysfibrinogenemic mutant that does not release FPA. At 14°C and physiologic solvent conditions (0.15 mol/L of NaCl, 0.015 mol/L of Tris buffer pH 7.4), the turbidity (350 nm) of rapidly polymerizing *αβ*-fibrin (thrombin 1 to 2 U/mL) plateaued in <6 min and formed a "coarse" matrix consisting of anastomosing fiber bundles (mean diameter 92 nm). More slowly polymerizing *αβ*-fibrin (thrombin 0.01 and 0.001 U/mL) surpassed this turbidity after ≥60 minutes and concomitantly developed a network of thicker fiber bundles (mean diameters 118 and 186 nm, respectively). Such matrices also contained networks of highly branched, twisting, "fine" fibrils (fiber diameters 7 to 30 nm) that are usually characteristic of matrices formed at high ionic strength and pH. Slowly polymerizing *β*-fibrin, like slowly polymerizing *αβ* fibrin, displayed considerable quantities of fine matrix in addition to an underlying thick cable network (mean fiber diameter 135 nm), whereas rapidly polymerizing *β*-fibrin monomer was comprised almost exclusively of wide, poorly anastomosed, striated cables (mean diameter 212 nm). Metz *β*-fibrin clots were more fragile than those of normal *β*-fibrin and were comprised almost entirely of a fine network. Metz fibrin could be induced, however, to form thick fiber bundles (mean diameter 76 nm) in the presence of albumin at a concentration (500 μmol/L) in the physiologic range and resembled a Metz plasma fibrin clot in that regard. The diminished capacity of Metz *β*-fibrin to form thick fiber bundles may be due to impaired use or occupancy of a polymerization site exposed by FPB release. Our results indicate that twisting fibrils are an inherent structural feature of all forms of assembling fibrin, and suggest that mature *β*-fibrin or *αβ*-fibrin clots develop from networks of thin fibrils that have the ability to coalesce to form thicker fiber bundles.

Thrombin-Catalyzed fibrin formation begins with the release of fibrinopeptide A (FPA) from the amino terminus of the A*α* chains of fibrinogen1, [2, 3, 4, 5] and is accompanied by the slower release of fibrinopeptide B (FPB) from B*β* chains. Reptilase, a snake venom enzyme from *Bothrops atrox*, removes only FPA,[6, 7, 8] release of which is sufficient for fibrin polymerization (α-fibrin) to occur.[7, 8, 9]

Mature fibrin clots evidently assemble from a network of thin protofibrils that subsequently, under physiologic solvent conditions, undergo lateral aggregation, causing increased fiber thickness.[10, 11, 12] Since 1947, two extreme forms of three dimensional fibrin networks, namely "fine" and "coarse," have been recognized.[13] The fine gel structure can be produced at high ionic strength and pH, is translucent and friable, and consists of a network of thin, highly branched, twisting fibers.[14] The coarse gel structure, which forms at or below physiologic ionic strength and pH, is opaque and easily synerized. Owing to a strong tendency for lateral association under such conditions, these matrices are characterized by thick fiber bundles, the thicknesses of which are reflected by turbidity measurements[10, 11, 12, 13,15, 16, 17, 18] and determined in part by the kinetics of fiber growth.[11,12,18,19] That is, slowly forming clots at physiologic pH and ionic strength tend to develop thicker fiber bundles than do more rapidly forming clots.[12,18,20]

Some investigators[2,3,5,8,21] have suggested that FPB release is essential for lateral fiber growth. Other studies, however, indicate that this is not the case,[10,11,16,22,23] since reptilase cleavage of FPA to form *α*-fibrin results in a coarse matrix whose cables are only moderately narrower than those formed by *αβ*-fibrin.[10,11,22] The light scattering studies of Müller and co-workers[24] also indicated that *α*-fibrin and *αβ*-fibrin were similar with respect to branching tendency and lateral aggregation. Thus, although FPB release is not strictly required for gelation or for lateral aggregation, its release may increase the rate and extent of lateral associations. [10,11,16] In additon, fiber slippage is reduced, fiber stiffness is increased, and branch points in *αβ*-fibrin fibers are probably reinforced by noncovalent bonding correlating with FPB release.[14,23,25] Mihalyi and Donovan[26] recently provided calorimetric data indicating that noncovalent interactions of the fibrin(ogen) D domains are enhanced by removal of FPB.

Preferential release of fibrinopeptide B by copperhead venom procoagulant enzyme (CVE)[27] is sufficient to cause normal fibrinogen to polymerize.[28,29] Based on their gross appearance, these clots tend to be fine at temperatures <25°C and are readily dissociated at 37°C.[28,29] Judging from light scattering measurements on fibrin clots formed at 20°C and 37°C, it apears that selective cleavage of FPB at low enzyme concentrations results in the highest branching density and the lowest degree of lateral aggregation.[24]

In this study, we used electron microscopy to investigate the three-dimensional structure of *β*-fibrin formed from normal fibrinogen and from the homozygous congenital fibrinogen abnormality known as fibrinogen Metz (A*α* Arg 16 → Cys).[30, 31, 32] To preserve the structures of these fragile fibrin clots, we prepared our material using the critical point drying technique[33] as recently used for the study of fine fibrin matrices.[14]

MATERIALS AND METHODS

Normal fibrinogen fraction 1-2 (>95% coagulable) and fibrinogen Metz fraction 1-2 were purified from citrated plasma by the method of Blombäck and Blombäck.[34] In some experiments, chromatographically purified normal peak 1 fibrinogen[33] was used. As assessed by the position of the fibrinogen band in $NaDodSO_4$-Polyacrylamide gel electrophoresis (PAGE) (5% acrylamide),[36,37] unreduced fibrinogen Metz molecules were devoid of polymeric forms and the preparation was ~95% pure.

Sulfhydryl titrations of various fibrinogen preparations were carried out either with Ellman's reagent, 5,5'-dithiobis (2-nitrobenzoic acid) (DTNB),[38] or with ^{3}H- or ^{l4}C-iodoacetic acid (specific activities 140 mCi/mmol and 11.1 mCi/mmol, respectively). After reaction with the iodoacetate, samples were

extensively dialyzed, dissolved in 10 mL of Aquasol-2 liquid scintillation cocktail (New England Nuclear, Boston), and radioactivity was subsequently determined in a Packard model 2425 spectrometer.

Freeze-dried human thrombin (H-l), a gift from Dr D. L. Aronson, was reconstituted in H_2O and stored frozen at a concentration of 100 U/mL. CVE was prepared as described by Herzig and co-workers[27] and had an activity of 33 TAME (Nα-p-tosyl-Larginine methyl ester) U/mL. Common chemicals were of reagent grade.

Fibrinogen samples for fibrinopeptide analyses were brought to a final concentration of 5 mg/mL in a buffer of 0.15 mol/L NaCl, 0.01 mol/L of Tris pH 7.2 ± 0.1, and incubated in small glass tubes after the addition of thrombin or CVE. Release of FPA and/or FPB from fibrinogen was measured after overnight incubation using the high-performance liquid chromatography (HPLC) chromatographic system described by Kehl and Henschen.[39] Specifically, the fibrinopeptides were analyzed with a Varian model 5040 HPLC apparatus on an Ultrasil ODS reverse-phase column (25 cm × 4.6 mm) (Rainin Instrument, Woburn, MA) using a linear gradient of acetonitrile (12% to 28%) buffered with 25 mmol/L of ammonium acetate pH 6.0.

$\alpha\beta$-Fibrin or β-fibrin was prepared by addition of thrombin or CVE (0.66 or 0.13 U/mL), respectively, at 14 ± 1°C, to normal fibrinogen, followed by overnight incubation at 14°C. Metz β-fibrin was generated at 14°C or 37°C by addition of CVE (0.66 U/mL) or thrombin (I to 5 U/mL). In some cases, bovine serum albumin (BSA) (500 μmol/L, final concentration; Sigma Chemical, St Louis) or $CaCl_2$ (5 mmol/L), or both were included in the clotting mixture.

HPLC determination of fibrinopeptides released from normal β-fibrin under these conditions revealed the expected presence of FPB and des-Arg FPB and ≤10% of the potentially available amount of FPA. Metz β-fibrin showed only FPB and des-Arg FPB. For those batches of CVE that contained Aα chain degradative activity, tosyl lysine chloromethyl ketone (Sigma Chemical) 10^{-4} mol/L, final concentration, was added to the clotting mixture prior to CVE addition to block this activity. Turbidity measurements at 350 nm on fibrin clots were carried out at 14 ± 1°C in a Gilford model 240 spectrophotometer equipped with a jacketed specimen holder.

Certain β-fibrin specimens were subjected to gel-sieving chromatography at 37°C to separate β-fibrin from a minor $\alpha\beta$-fibrin contaminant.[29] In brief, following the incubation period with CVE, the clot was overlaid with 1 mmol/L of phenylmethylsufonyl fluoride (PMSF) in buffer and incubated in the presence of this reagent for at least 2 hours. The fibrin was then dissociated by being warmed to 37°C, mixed with an equal volume of 0.3 mol/L of NaCl, 0.03 mol/L of Tris buffer pH 7.4 ± 0.1 PMSF 10^{-4} mol/L, and gel-filtered at 37°C through a Sepharose 2B column equilibrated in this same buffer. Early eluting fractions containing the $\alpha\beta$-fibrin contaminant were discarded, whereas fractions containing "β-fibrin monomer" eluting at a concentration above six-tenths of the β-fibrin peak height were pooled and stored frozen at −30°C at concentrations ranging from 400 to 800 μg/mL. For electron microscopy or turbidity measurements, aliquots of β-fibrin monomer were thawed at 37°C for 30 minutes, diluted 1:1 with H_2O, and then incubated at 14°C for the desired amount of time. Preparations were monitored by $NaDodSO_4$-PAGE[36,37] to verify whether anticipated fibrinopeptide cleavages had occurred and to determine if other proteolytic attack had occurred (eg, on Aα chains).

Samples of purified fibrin for negative staining electron microscopy were formed at 14 ± 1°C as 50-μL drops (50 to 500 μg/mL) in a Petri dish that had been humidified with a moist sponge, incubated for 16

to 18 hours with thrombin or CVE, picked up on glow discharged carbon films, and then negatively contrasted with 2% (wt/vol) uranyl sulfate. For processing by the critical point drying technique, clots were picked up on glow-discharged carbon-coated 200-mesh copper grids, fixed with glutaraldehyde (2.5%, vol/vol) in 0.1 mol/L of HEPES buffer pH 7.0, containing 0.2% (wt/vol) tannic acid, washed several times with H_2O, stained with 0.5% (wt/vol) uranyl acetate, and washed again with H_2O.[14] The specimen was then dehydrated in graded ethanol solutions (20% to 100%, vol/vol) and CO_2 critical point dried[33] using a Tousimis model 780A critical point drying apparatus (Tousimis Scientific Instruments, Rockville, MD).

Plasma fibrin clots were prepared from blood that had been drawn into a plastic syringe, immediately transferred to a centrifuge tube, and then centrifugea at 3,000 g for 3 to 5 minutes to remove cellular elements. The supernatant plasma was incubated overnight at room temperature, and the resulting clot was synerized, washed extensively with saline, and fixed overnight at 4°C in 2% (wt/vol) glutaraldehyde solution in 0.1 mol/L of phosphate buffer pH 7.2. Metz fibrin clots were also prepared without syneresis from purified Metz fibrinogen at 2 mg/mL. The fixed preparation was incubated for 90 minutes with 2% osmium tetroxide in 0.1 mol/L of phosphate buffer, dehydrated in graded ethanol solutions, and embedded in Spurr's low-viscosity medium.[40] Thin sections were prepared using a diamond knife and a Reichert Ultracut ultramicrotome and stained with 5% aqueous uranyl acetate and Sato's lead citrate solution.[41]

Electron microscopy was performed with a Philips model 400 transmission electron microscope at 60 to 120 kV or with the University of Wisconsin high-voltage (1,000 kV) electron microscope at Madison, WI. Stereo images were made at magnifications of 5,000x to 22,000x at tilt angles of 3° to 6°.

RESULTS

We prepared *β*-fibrin at 14°C to minimize cleavage of FPA by CVE,[28] and we used this same temperature for polymerization of other forms of fibrin. The standard way of processing fibrin for transmission electron microscopy (TEM) is to pick up a clot sample by passing a carbon-coated grid through a fibrin clot. The grid surface is washed subsequently with buffer and uranyl sulfate and then air dried. Samples processed in this way have been suitable for observing the structure of a normal coarse fibrin matrix[42,43] and for characterizing the structure of certain abnormal fibrins such as fibrinogen Paris I.[44] The Metz clot structure and that of *β*-fibrin was so fragile, however, that at best we found discontinuous short strands and occasionally anastomosing fiber bundles and thin fibrils adherent to the underlying substrate. To preserve the three-dimensional structure of this type of clot, we processed the sample using the critical point drying procedure.[33] This technique has been used for demonstrating previously unrecognized features of fine clot matrices.

αβ-Fibrin.

Images of critical point dried, rapidly polymerizing *αβ*-fibrin (thrombin, 1 U/mL) formed at 14°C under physiologic conditions (ie, I ~0.15, pH 7.4), revealed a coarse matrix consisting predominantly of twisted anastomosing cables (Fig 1A, Table 1). These cables showed typical cross-striations (~22 nm period) when viewed at a higher magnification than that shown in Fig 1 (data not shown).*

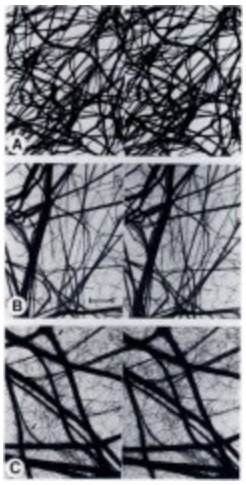

Fig 1. Stereo images by transmission electron microscopy (TEM) of *αβ*-fibrin (500 *μ*g/mL) prepared by incubation overnight at 14°C under "coarse clot" buffer conditions (0.15 mol/L of NaCl. 0.015 mol/L of Tris buffer, pH 7.4) at the following thrombin concentrations: (A) 1 U/mL; (B) 0.01 U/mL; (C) 0.001 U/mL. Bar = 1,000 nm. The arrows in (C) indicate loosely packed fiber bundles.

Table 1. Fiber Diameter of Thick Fiber Bundles of *αβ*-Fibrin and *β*-Fibrin

Preparation	**Concentration (*μ*g/mL)**	**n***	**Fiber Diameter (nm)**		
			Mean	**SD**	**Range**
αβ-Fibrin (thrombin, 2 U/mL)	50	36	83	±37	50–170
αβ-Fibrin (thrombin, 1 U/mL)	500†	89	92	±39	36–260
αβ-Fibrin (thrombin, 0.01 U/mL)	500	43	118	±59	35–256
αβ-Fibrin (thrombin, 0.001 U/mL)	500	36	186	±90	60–536
β-Fibrin monomer	355	55	212	±80	40–520
β-Fibrin (CVE, 0.66 U/mL)	500	36	87	±30	35–170
β-Fibrin (CVE, 0.13 U/mL)	500	48	135	±73	35–421
Metz *β*-fibrin + albumin + Ca^{2+}	500	29	76	±32	39–194

In matrices containing significant amounts of both "fine" and "coarse" networks, there appeared to be no sharp size transitions in the progression from thin fibers in the fine matrix (7 to 30 nm in diameter) toward thicker fibers approaching the mean values. For purposes of this analysis, we defined the diameter of a coarse fiber bundle as ≥35 nm.

*Number of fibers measured.

†Owing to the thickness of the clot in the critical point dried specimen, it seemed tenuous to assume that areas selected for fiber measurement were representative of the fiber population in the clot. For that reason, we also prepared thin sections of an imbedded specimen under these same conditions. The fiber diameter determined from this type of specimen preparation was 92 ± 26 nm, range 37–150 nm. SD and range of values were lower because we used only the minimum cross-sectional diameter of any given fiber to avoid including measurement of tangential or oblique sections of fibers in our calculations.

At a 100-fold lower thrombin concentration (0.01 U/mL), the rate of fibrin polymerization was considerably slowed (Fig 3); nevertheless, the clot ultimately developed considerably greater turbidity than fibrin formed at 1 U/mL. These observations confirm studies indicating that slow rates of fibrin

polymerization favor higher degrees of lateral aggregation (ie, thicker fiber bundles).[12,18,20] At a thrombin concentration of 0.001 U/mL, clot development proceeded even less rapidly than at 0.01 U/mL although the turbidity eventually exceeded that of rapidly polymerizing *αβ*-fibrin. $NaDodSO_4$-PAGE analysis of fibrin specimens taken at the time of fixation for critical point drying, indicated that complete FPA release had occurred in all cases, but that in the specimen prepared at a thrombin concentration of 0.001 / mL, only 50% of FPB had been released.

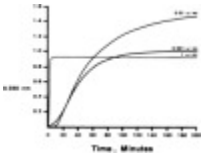

Fig 3. Turbidity measurements on *αβ*-fibrin. These experiments were carried out under the same conditions described in Fig 1. Thrombin was added to a final concentration of 1 U/mL. 0.01 U/mL, or 0.001 U/mL; absorbance (A_{350} nm) was monitored as a function of time.

Consistent with turbidity measurements, fibrin formed at 0.01 U/mL or 0.001 U/mL revealed a network predominantly composed of large anastomosing fiber bundles that tended to be thicker than those from rapidly polymerized *αβ*-fibrin (Fig 1). In addition to the thick cable network, however, there was also a prominent network of thinner fibrils. This second type of matrix was most prominent at the lowest thrombin concentration (0.001 U/mL) and consisted of highly branched, twisting fibrils (Fig 4) that appeared to entrap and merge with large fiber bundles. The thick cables forming under this latter condition were composed of loosely packed fibrils (arrows, Fig 1C) and did not display the striations typical of more tightly packed bundles.

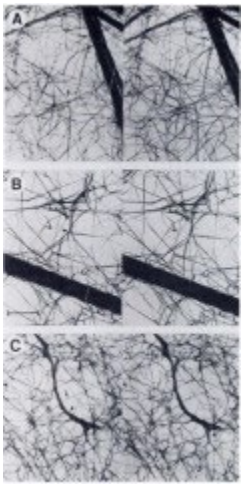

Fig 4. Stereo images of fibrin specimens showing extensive fine fibril networks. (A) *αβ*-fibrin (TEM); thrombin 0.001 U/mL; (B) *β*-fibrin (TEM); copperhead venom procoagulant enzyme 0.13 U/ml; (C) thrombin-generated Metz *β*-fibrin monomer (HVEM). Bar = 500 nm.) Arrows indicate a typical twisting thin fibril. Arrowhead (C) points to a relatively short fiber bundle within the predominantly thin fiber matrix.

β-Fibrin.

β-Fibrin gels formed at 14°C can be dissociated by being warmed to 37°C, and the resulting *β*-fibrin monomer can subsequently be polymerized by incubation at room temperature or below.[28,29] This process can be carried out repeatedly on material that has been inactivated with PMSF. Turbidity measurements on such a *β*-fibrin monomer preparation (Fig. 5) indicated that the onset of polymerization was more rapid than that of *β*-fibrin formed by direct addition of CVE (Fig 6). The initial rate of turbidity rise of *β*-fibrin forming at the higher CVE concentration (0.66 U/mL), however, was about the same as the value for *β*-fibrin monomer extrapolated to a concentration of 500 μg/mL (ie, 0.06l/min *v* 0.065/min). Electron micrographs of the *β*-fibrin monomer clot showed a network of twisting, occasionally anastomosing cables (Fig 7A). The mean fiber diameter was greater than in any other type of *β*-fibrin or *αβ*-fibrin matrix (Table l).

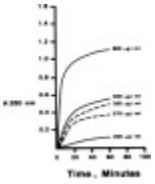

Fig 5. Turbidity measurements on *β*-fibrin monomer. Repoly merization at 14°C under standard buffer conditions of *β*-fibrin monomer that had been dissociated at 37°C (—) or further processed after dissociation at 37°C by molecular exclusion chromatography to remove *αβ*-fibrin contamination (—). The curves developed by chromatographically processed *β*-fibrin monomer are in register with those of unprocessed *β*-fibrin monomer, suggesting that a small amount of *αβ*-fibrin contamination does not materially change the structure of the matrix that forms.

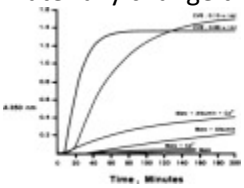

Fig 6. Turbidity measurements on *β*-fibrin (500 μg/mL). CVE additions, 0.66 or 0.13 U/mL, to normal fibrinogen at 14°C were made under the same buffer conditions described in Fig 1. Metz *β*-fibrin was incubated with thrombin (5 U/mL) at 14°C and allowed to polymerize under the following conditions: Metz + buffer; Metz + $CaCl_2$, 5 mmol/L; Metz + albumin, 500 μmol/L; Metz + albumin. 500 μmol/L + $CaCl_2$, 5 mmol/L.

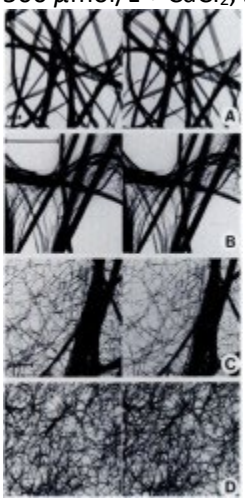

Fig 7. Stereo images of *β*-fibrin clots sampled after incubation overnight at 14°C under the same buffer conditions described in Fig 1. (A) *β*-fibrin monomer (high-voltage electron microscopy HVEM) 355 μg/mL; (B) *β*-fibrin (TEM) 500 μg/mL; copperhead venom procoagulant enzyme (CVE) 0.66 U/mL; (C) *β*-fibrin (TEM) 500 μg/mL; CVE. 0.13 U/mL; (D) thrombin-generated Metz *β* fibrin monomer (TEM), 500 μg/mL. Bars = 1,000 nm. Arrow (C) indicates a loosely packed fiber bundle.

β-Fibrin produced by addition of CVE (Fig 7) formed a network of thick cables frequently displaying periodic striations (see footnote, page 1075) typical of *α*-fibrin or *αβ*fibrin bundles. The fiber bundles in these networks, like the *β*-fibrin monomer network, anastomosed only occasionally relative to *αβ*-fibrin clots. At the highest CVE level (0.66 U/mL), the matrix revealed occasional areas of fine, fibrillar networks, usually bridging between thick cables (Fig 7B) or appearing to represent an unraveled or frayed portion of a thick fiber bundle. At a lower CVE level (0.13 U/mL), fiber bundles in the matrix were more loosely packed (Fig 7C, arrow) and wider than those formed at the higher CVE concentration. In addition to the predominant thick cable structure, this clot showed a considerable network of fine twisting fibrils (Fig 7C and Fig 4B).

Metz β-fibrin.

Metz *β*-fibrin is more transparent, less viscous, and more easily disrupted than normal *β*-fibrin. In contrast to normal, Metz *β*-fibrin formed by direct addition of thrombin or CVE at 14°C or that formed at 14°C from Metz *β*-fibrin monomer solutions (ie, first incubated with thrombin at 37°C), revealed a matrix comprised almost entirely of thin, twisting, and highly branched fibrils (Figs 4C and 7D) that occasionally coalesced to form somewhat thicker, relatively short, uneven bundles. These observations are consistent with the very low turbidity recorded at 350 nm (Fig 6).

To evaluate the type of Metz fibrin matrix formed in vivo, we prepared fibrin directly from native plasma and examined thin sections by electron microscopy (Fig 2). Normal fibrin yielded the expected thick, striated cables (Fig 2A, arrow), whereas Metz fibrin yielded loosely packed fiber bundles that frequently were sufficiently in register to yield a striated pattern (Fig 2B, arrow). Fibrin aggregation is well known to accelerate in plasma,[45] and this is due in part to effects related to the presence of albumin and IgG.[46,47] The accelerating effect is also accompanied by increased clot turbidity that is attributable, at least in part, to the presence of albumin or IgG, or both,[47] and Ca^{2+}.[48,49] To provide an explanation for the more mature structure of Metz plasma fibrin relative to purified thrombin-generated or CVE-generated Metz fibrin, we attempted to induce thick fibril formation by allowing thrombin-generated Metz fibrin to polymerize in the presence of albumin (500 μmol/L) or 5 mmol/L of $CaCl_2$, or both (Fig 6). Measurements in the presence of albumin showed increased turbidity developing slowly over several hours; this effect was even more marked when 5 mmol/L of $CaCl_2$ was also present, although addition of $CaCl_2$ alone to Metz fibrin had little effect (Figs 6 and 2C). Examination and measurement of critical point dried fibrin specimens confirmed that increased thick bundle formation had occurred in albumin-containing specimens (cf Fig 2C and 2D). The thick bundles, like the fine fibrils, had a tendency to twist, but periodic striations were not observed. As assessed by TEM of thin sections, thick fiber bundle formation could also be induced in Metz *β*-fibrin formed at a concentration approximating that in plasma (ie, 2 mg/mL) (data not shown).

Comparison of the ultrastructure of a Metz plasma fibrin clot with Metz fibrin formed in the presence of albumin or Ca2+ or both (TEM). (A) Thin section of a normal plasma fibrin clot; (B) thin section of a Metz

plasma clot; bar = 500 nm (A and B); (C) critical point dried specimen of Metz fibrin prepared in the presence of 5 mmol/L of CaCl2; (D) critical point dried specimen of Metz fibrin prepared with albumin 500 µmol/L and CaCI2 5 mmol/L; bar = 500 nm (A and B). Arrows (A and B) point to periodic striations that occur in thick fiber bundles.

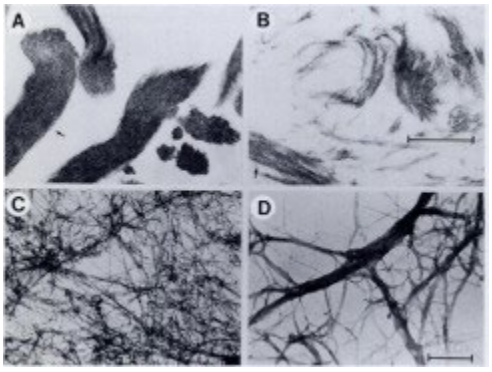

Fig 2. Comparison of the ultrastructure of a Metz plasma fibrin clot with Metz fibrin formed in the presence of albumin or Ca^{2+} or both (TEM). (A) Thin section of a normal plasma fibrin clot; (B) thin section of a Metz plasma clot; bar = 500 nm (A and B); (C) critical point dried specimen of Metz fibrin prepared in the presence of 5 mmol/L of $CaCl_2$; (D) critical point dried specimen of Metz fibrin prepared with albumin 500 μmol/L and $CaCl_2$ 5 mmol/L; bar = 500 nm (A and B). Arrows (A and B) point to periodic striations that occur in thick fiber bundles.

Sulfhydryl content.

Gel electrophoretic analysis of fibrinogen Metz, as well as electron micrographs of negatively contrasted Metz fibrinogen (not shown), revealed that Metz molecules were monomolecular and thus were not joined by intermolecular covalent (ie, disulfide) bridges. To investigate further whether the cysteine residues in fibrinogen Metz at position 16 were oxidized to disulfides, we evaluated the titratable sulfhydryl (SH) content using Ellman's reagent.[38] Normal fibrinogen, which has no free SH groups,[50] and Metz fibrinogen yielded <0.2 mol of titratable SH groups per mole of fibrinogen. We also used a more sensitive technique to detect the presence of SH groups by labeling with ^{3}H or ^{14}C iodoacetic acid. With this technique, the titratable SH content of Metz fibrinogen as well as that of normal peak 1 fibrinogen was 0.01 to 0.02 mol of SH/mol of fibrinogen.

DISCUSSION

Although many EM studies have been made of the structure of *α*-fibrin and *αβ*-fibrin, to our knowledge none have reported on the ultrastructure of *β*-fibrin. By using the critical point drying technique to process fibrin clots, we were able to preserve clot structure and obtain high-quality, detailed stereo images of *β*-fibrin and Metz *β*-fibrin and Metz *β*-fibrin clot networks. Our findings, coupled with turbidometric analyses, permitted a comparison of the structure of *αβ*-fibrin with that of *β*-fibrin and Metz *β*-fibrin.

It is clear from our present findings that release of FPB alone can give rise to clots whose features resemble those of *α*-fibrin in several important ways: (a) Both types of fibrin tend to form thick twisting cables displaying typical periodic cross-striations under physiologic buffer conditions. When polymerization takes place relatively slowly, both types of fibrin develop fine fibrillar network structures

in addition to a relatively thicker cable network. The latter observation is consistent with previous studies indicating that fiber thickness is determined in part by the kinetics of fiber growth.[11,12,18,19,20] (b) The fibrils from both types of fibrin show the characteristic twisting described by Müller and colleagues[14] for fine clots. Regions containing fine fibrillar matrix structures, whether derived from normal (*β*-fibrin or *αβ*-fibrin) or Metz *β*-fibrin, are not easily distinguishable from the fine matrix formed by *αβ*-fibrin at high ionic strength/pH[14] or in a slowly polymerizing system under physiologic conditions (this study).

Twisting is not only a characteristic of native fibrin fibrils (ref. 14 and this study), but is also a prominent feature of microcrystals and fibrin clots prepared from enzymatically modified fibrinogen.[51,52] We infer from those results and from our present observations that fiber twisting is an inherent feature of fibrin assembly when polymerization is initiated by release of either FPA or FPB.

Slowly polymerizing *αβ*-fibrin or *β*-fibrin networks contain fine fibrillar substructures that are superimposed on and merge with thick, loosely packed fiber bundle networks. Such structures evidently reflect an intermediate phase of fibrin assembly during which thick cables coalesce from a fine fibrillar matrix to form the mature anastomosing cable network. This observation is consistent with the observations that under physiologic conditions mature fibrin assembly develops over a relatively long time[23] from protofibrils that subsequently undergo lateral aggregation to form thick fiber bundles.[10,11,12] The precise mechanism by which this assembly process takes place is not yet known.

Clot turbidity is reportedly a function of the second power of fiber diameter.[15,17,53] Therefore, such measurements are sensitive to the presence of thick fiber bundles but not to fine fiber networks. The widest cable structures we observed occurred in the coarse *β*-fibrin monomer clots, yet these gels ultimately developed lower turbidity than did the rapidly polymerizing coarse *αβ*-fibrin matrix or any other *β*-fibrin or *αβ*-fibrin network having lower mean fiber widths (Table 1). This seemingly paradoxical phenomenon may indicate that light scattering per se is not strictly a function of fiber width but may also be related to factors such as tightness of fiber packing, branching, etc. Further studies combining electron microscopy with detailed physical and rheological measurements of clot properties should be most useful in clarifying this issue.

In contrast to turbidity, measurement of clot permeability is a reflection of pore size, coarse clots having greater permeability than fine clots.[15,17,18,19,20] Shah and colleagues[17,18] observed that the permeability of fibrin formed at a low thrombin concentration did not rise in proportion to the increase in fiber thickness calculated from turbidity measurements. Such observations are consistent with our present demonstration that slow polymerization (*αβ*-fibrin or *β* fibrin) is accompanied not only by increased fiber thickness, but also by the formation of fine fiber networks. Deductions on clot matrix structure based on turbidity and permeability measurements depend on the assumption of a uniform population of network fibers. This is evidently not the case (ref. 17 and this study), especially under circumstances that are intermediate to the extremes of fine and coarse fiber network formation.

Release of FPA and FPB exposes independent binding sites in the NH_2-terminal region of the molecule which appear to function cooperatively in the aggregation pro-cess.[28,29] Release of FPA exposes the “A” site, which becomes aligned with the complementary “a” site in the D domain of another molecule.[5,21] Similarly, FPB release evidently exposes a “B” polymerization site,[28,29] efficient utilization of which by the complementary “b” site may depend on proper alignment of two D domains in an *αβ*-fibrin polymer.[21] Substitution of cysteine for arginine at A*α* 16 in fibrinogen Metz evidently impairs this

process because Metz *β*-fibrin, unlike normal *β*-fibrin, has only a weak tendency for lateral aggregation. This impairment may be due to the existence of a disulfide bridge at A*α* 16.[54] The substitution may impose conformational or steric changes that interfere with proper occupancy or orientation of the polymerization site unmasked by release of FPB, thus impairing optimal alignment of fibrils into bundles. Further study of this impairment may lead to new insights into the exact location of the region involved in the ability of fibrin to form lateral associations with other fibrin molecules.

In contrast to purified Metz fibrin, the Metz plasma clot was less fragile, could be synerized, and showed a considerable degree of lateral aggregation, even to the extent of forming easily discernible periodic striations (Fig 7). This "improvement" in Metz clot structure is not surprising since fibrin aggregation in plasma is associated with increased clot turbidity and increased lateral fiber aggregation.[47] When Metz fibrin was formed at concentrations approaching that in plasma or at an albumin concentration in the physiologic range (500 μmol/L), we were able to induce an increased degree of lateral fiber association. This effect was even more pronounced when Ca^{2+} was also present. We believe that the differences between purified Metz *β*-fibrin and plasma Metz *β*-fibrin structure are largely attributable to the fact that the plasma environment favors lateral fiber growth, due in part to the relative concentration of fibrinogen and to albumin or IgG.[46,47] Other plasma factors contributing to the strength and structure of the Metz plasma clot (eg, crosslinking) remain to be explored. In this regard, the Metz subject is not a severe or spontaneous bleeder, although she often bleeds for prolonged periods from venipuncture sites and is a habitual aborter.[30] Perhaps the relatively mild clinical bleeding that she manifests reflects the effect that the plasma environment has in enhancing fibrin clot formation.

ACKNOWLEDGMENT

We are most grateful to Julie Erickson for outstanding secretarial assistance, to Vicki Ainslie for technical assistance, and to Joyce A. Mitchell for graphics services.

REFERENCES

1 Sheraga HA. **Laskowski M Jr: The fibrinogen-fibrin conversion.** *Adv Prot Chem*, 12 (1957), p. 1

2 Laurent TC, Blombäck B. **On the significance of the release of two different peptides from fibrinogen during clotting.** *Acta Chem Scand*, 12 (1958), p. 1875

3 Laki K, Gladner JA. **Chemistry and physiology of the fibrinogen-fibrin transition.** *Physiol Rev*, 44 (1964), p. 127

4 Doolittle RF. **Structural aspects of the fibrinogen to fibrin conversion.** *Adv Prot Chem*, 27 (1973), p. 1

5 Blombäck B, Hessel B, Hogg D, Therkildsen L. **A two-step fibrinogen-fibrin transition in blood coagulation.** *Nature*, 275 (1978), p. 501

6 Blombäck B. **Studies on the action of thrombic enzymes on bovine fibrinogen as measured by N-terminal analysis.** *Ark Kemi*, 12 (1958), p. 321

7 Blombäck B, Blombäck M, Nilsson IM. **Coagulation studies on "reptilase," an extract of the venom from Bothrops jararaca.** *Thromb Diath Haemorh*, 1 (1957), p. 76

8 Blombäck B, Laurent TC. **N-terminal and light-scattering studies on fibrinogen and its transformation to fibrin.** *Ark Kemi*, 12 (1958), p. 137

9 Shainoff JR, Page IH. **Significance of cryoprofibrin in the fibrinogen to fibrin conversion.** *J Exp Med*, 116 (1962), p. 687

10 Hantgan R, Fowler W, Erickson H, Hermans J. **Fibrin assembly: A comparison of electron microscopic and light scattering results.** *Thromb Haemostas*, 44 (1980), p. 119

11 Hantgan R, McDonagh J, Hermans J. **Fibrin assembly.** *Ann NY Acad Sci*, 408 (1983), p. 344
12 Wolfe JK, Waugh DF. **Relations between enzymatic and association reactions in the development of bovine fibrin clot structures.** *Arch Biochem Biophys*, 211 (1981), p. 125
13 Ferry JD, Morrison PR. **Preparation and properties of serum and plasma proteins. VIII. The conversion of human fibrinogen to fibrin under various conditions.** *J Am Chem Soc*, 69 (1947), p. 388
14 Müller MF, Ris H, Ferry JD. **Electron microscopy of fine fibrin clots and coarse fibrin films.** *J Mol Biol*, 174 (1984), p. 369
15 Carr J Jr, Shen LL, Hermans J. **Mass-length ratio of fibrin fibres from gel permeation and light scattering.** *Biopolymers*, 16 (1977), p. 1
16 Hantgan R, Hermans J. **Assembly of fibrin: A light scattering study.** *J Biol Chem*, 254 (1979), p. 11272
17 Shah G, Ferguson IA, Dhall TZ, Dhall DP. **Polydispersion in the diameter of fibres in fibrin networks consequences on the measurement of mass-length ratio by permeability and turbidity.** *Biopolymers*, 21 (1982), p. 1037
18 Shah G, Nair CH, Dhall DP. **Physiological studies on fibrin network structure.** *Thromb Res*, 40 (1985), p. 181
19 Blombäck B, Okada M. **Fibrin gel structure and clotting time.** *Thromb Res*, 25 (1982), p. 51
20 Rosser RW, Roberts WW, Ferry JD. **Rheology of fibrin clots. IV. Darcy constants and fiber thickness.** *Biophys Chem*, 7 (1977), p. 153
21 Olexa SA, Budzynski AZ. **Evidence for four different polymerization sites involved in human fibrin formation.** *Proc Natl Acad Sci USA*, 77 (1980), p. 1374
22 Shen LL, Hermans J, McDonagh J, McDonagh RP. **Role of fibrinopeptide B release: Comparison of fibrins produced by thrombin and ancrod.** *Am J Physiol*, 232 (1977), p. H629
23 Bale MD, Müller MF, Ferry JD. **Rheological studies of creep and creep recovery of unligated fibrin clots: Comparison of clots prepared with thrombin and ancrod.** *Biopolymers*, 24 (1985), p. 461
24 Müller M, Lasarcyk H, Burchard W. **Fibrinogen-fibrin transformation: II. Influence of temperature, pH and of various enzymes on the intermediate structures.** *Int J Biol Macromol*, 3 (1981), p. 19
25 Müller MF, Ferry JD. **Stress relaxation in fine fibrin films: Comparison of films prepared with thrombin and ancrod.** *Biopolymers*, 23 (1984), p. 2311
26 Mihalyi E, Donovan JW. **Clotting of fibrinogen. II. Calorimetry of the reversal of the effect of calcium on clotting with thrombin and with ancrod.** *Biochemistry*, 24 (1985), p. 3443
27 Herzig RH, Ratnoff OD, Shainoff JR. **Studies on a procoagulant fraction of southern copperhead venom: The preferential release of fibrinopeptide B.** *J Lab Clin Med*, 76 (1970), p. 451
28 Shainoff JR, Dardik BN. **Fibrinopeptide B and aggregation of fibrinogen.** *Science*, 204 (1979), p. 200
29 Shainoff JR, Dardik BN. **Fibrinopeptide B in fibrin assembly and metabolism: Physiologic significance in delayed release of the peptide.** *Ann NY Acad Sci*, 408 (1983), p. 254
30 Soria J, Soria C, Samama C, Poirot E, Kling C. **Fibrinogen Troyes—Fibrinogen Metz. Two new cases of congenital dysfibrino genemia.** *Thromb Diath Haemorrh*, 27 (1972), p. 619
31 Soria J, Soria C, Boulard C. **Anomalie de structure du fibrinogène "Metz," localisée sur la chaine α (A) de la molecule.** *Biochimie*, 54 (1972), p. 415
32 Soria J, Soria C, Samama M, Henschen A, Southan C. **Detection of fibrinogen abnormality in dysfibrinogenemia: Special report on fibrinogen Metz characterization by an amino acid substitution located at the peptide bond cleaved by thrombin.**
Henschen A, Graeff H, Lottspeich F (Eds.), *Fibrinogen. Recent Biochemical and Medical Aspects*, de Gruyter, New York (1982), p. 129
33 Anderson TF. **Techniques for the preservation of three dimensional structure in preparing specimens for the electron microscope.** *Trans NY Acad Sci*, 13 (1951), p. 130
34 Blombäck B, Blombäck M. **Purification of human and bovine fibrinogen.** *Ark Kemi*, 10 (1956), p. 415

35 Mosesson MW, Finlayson JS. **Subfractions of human fibrinogen—Preparation and analysis.** *J Lab Clin Med*, 62 (1963), p. 663
36 Weber K, Osborn M. **The reliability of molecular weight determinations by dodecyl sulfate Polyacrylamide gel electrophoresis.** *J Biol Chem*, 244 (1969), p. 4406
37 Laemmli UK. **Cleavage of structural proteins during the assembly of the head of bacteriophage T_4.** *Nature*, 227 (1970), p. 680
38 Ellman GL. **Tissue sulfhydryl groups.** *Arch Biochem Biophys*, 82 (1959), p. 70
39 Kehl M, Henschen A. **Characterisation of the peptides released at the fibrinogen-fibrin conversion using high performance liquid chromatography.** Lottspeich F, Henschen A, Hupe K-P (Eds.), *HPLC in Protein and Peptide Chemistry*, de Gruyter, New York (1981), p. 339
40 Spurr AR. **A low-viscosity epoxy resin embedding medium for electron microscopy.** *J Ultrastr Res*, 26 (1969), p. 31
41 Sato T. **A modified method for lead staining of thin sections.** *J Electron Microsc*, 17 (1968), p. 158
42 Pouit L, Marcille G, Suscillon M, Hollard D. **Etude en microscopie électronique de différentes ètapes de la fibrinoformation.** *Thromb Diath Haemorrh*, 27 (1972), p. 559
43 Kay D, Cuddigan J. **The fine structure of fibrin.** *Br J Haematol*, 13 (1967), p. 341
44 Mosesson MW, Feldmann G, Ménaché D. **Electron microscopy of fibrin Paris I.** *Blood*, 56 (1980), p. 80
45 Ratnoff OD. **An accelerating property of plasma for the coagulation of fibrinogen by thrombin.** *J Clin Invest*, 33 (1) (1954), p. 175
46 Wilef J, Gladner JA, Minton AP. **Acceleration of fibrin gel formation by unrelated proteins.** *Thromb Res*, 37 (1985), p. 681
47 Galanakis DK, Lane BP, Simon SR: Albumin modulates lateral assembly of fibrin polymers: Evidence of enhanced fine fibril formation and of unique synergism with fibrinogen. Biochemistry (in press)
48 Boyer MH, Shainoff JR, Ratnoff OD. **Acceleration of fibrin polymerization by calcium ions.** *Blood*, 39 (1972), p. 382
49 Furlan M, Rupp C, Beck EA, Svendsen L. **Effect of calcium and synthetic peptides on fibrin polymerization.** *Thromb Haemostas*, 47 (1982), p. 118
50 Henschen A. **Number and reactivity of disulfide bonds in fibrinogen and fibrin.** *Ark Kemi*, 22 (1964), p. 355
51 Hewat EA, Tranqui L, Wade RH. **Structural study of modified fibrinogen microcrystals by electron microscopy.** *J Mol Biol*, 161 (1982), p. 459
52 Hewat EA, Tranqui L, Wade RH. **Electron microscope structural study of modified fibrin and a related modified fibrinogen aggregate.** *J Mol Biol*, 170 (1983), p. 203
53 Carr ME, Hermans J. **Size and density of fibrin fibers from turbidity.** *Macromolecules*, 11 (1978), p. 46
54 Mosesson MW, Siebenlist KR, DiOrio JP, Hainfeld JF, Wall JS, Soria J, Soria C, Samama M. **Evidence that proximal NH_2terminal portions of fibrinogen Metz (Aα 16 Arg → Cys) Aα chains are oriented in the same direction.** Müller-Berghaus G, ScheefersBorchel U, Selmayr E, Henschen A (Eds.), *Fibrinogen and Its Derivatives*, Elsevier, New York (1986), p. 3